Supporting Information

Martino et al. 10.1073/pnas.1221602110

SI Materials and Methods

Growth Factors. All growth factors (GFs) were purchased in their mature forms, highly pure (> 95% pure), carrier-free, and lyophilized. VEGF-A121, VEGF-B, VEGF-C, and PDGF-DD were purchased from R&D Systems. VEGF-A165, FGF-2, and PDGF-BB were purchased from Invitrogen. FGF-1, FGF-4, FGF-5, FGF-6, FGF-7, FGF-8, FGF-9, FGF-10, FGF-18, bone morphogenetic protein (BMP)-2, BMP-7, TGF-β1, TGF-β2, TGF-β3, EGF, heparin-binding (HB)-EGF, PDGF-AA, PDGF-AB, PDGF-CC, placenta growth factor (PlGF)-1, PlGF-2, PlGF-3, insulin-like growth factor (IGF)-I, IGF-II, insulin-like growth factor binding protein (IGFBP)-1, IGFBP-2, IGFBP-3, IGFBP-4, IGFPB-5, nerve growth factor (NGF), neutrophin 3 (NT-3), and BDNF were purchased from PeproTech. Except for VEGF-A165, PDGF-DD, VEGF-C, TGF-β1, TGF-β2, TGF-β3, BMP-7, IGFBP-2, and IGFBP-4, which were produced in eukaryotic cells, all GFs were produced in *Escherichia coli* and thus were not glycosylated. All GFs were reconstituted and stored according to the provider's instructions to regain full activity and prevent loss of protein.

Detection of GF–Fibrinogen Binding. ELISA plates (Nunc MaxiSorp; Thermo Fisher Scientific) were coated with 50 nM GF for 1 h at 37 °C and then blocked with 2% (wt/vol) BSA in PBS-Tween 20 (PBS-T, 0.05%) for 1 h at room temperature. Then wells were washed with PBS-T and further incubated with 100 nM fibrinogen depleted of fibronectin, plasminogen, and von Willebrand factor in PBS-T with 0.1% BSA (Enzyme Research Laboratories) for 45 min at room temperature. After three washes with PBS-T, wells were incubated with anti-fibrinogen antibody conjugated to HRP (ab7539; Abcam) for 45 min. After washing, antibody was detected with tetramethylbenzidine substrate by measuring the absorbance at 450 nm.

Release of GF from Fibrin Matrix. Fibrin matrices were generated with human fibrinogen as described previously (1). In brief, fibrin matrices were generated with 8 mg/mL fibrinogen, 2 U/mL human thrombin (Sigma-Aldrich), 4 U/mL factor XIIIa (Fibrogammin; Behring), 5 mM calcium chloride, and 500 ng/mL GF. Fibrin gels were polymerized at 37 °C for 1 h and transferred into 24-well Ultra Low Cluster plates (Corning) containing 500 μL of buffer (20 mM Tris·HCl, 150 mM NaCl, and 0.1% BSA; pH 7.4). A control well that served as a 100% released control contained only the GF in 500 μL of buffer. Every 24 h, buffers were removed, stored at −20 °C, and replaced with fresh buffer. For the 100% released control well, 20 μL of buffer was removed each day and stored at −20 °C. After 7 d, the cumulative release of GF was quantified by ELISA (DuoSet; R&D Systems), using the 100% released control as a reference. Matrices containing FGF-2 and PlGF-2 were digested at day 7 by the addition of 0.05 U of plasmin (Roche) in the release buffer.

Production of the Fibrin(ogen) Fragments. cDNAs encoding for human fibrinogen fragments were purchased from GenScript and inserted in the expression vector pGEX-6P-1 for expression as a GST fusion protein supplemented with a C terminus 6X His tag. GST-fibrinogen fragments were generated in BL21 *Escherichia coli* and purified by GST affinity chromatography (ÄKTA Explorer; GE Healthcare), as described previously (1). The GST tags were removed using PreScission protease (GE Healthcare) at 2 U/mg of fusion protein. Cleaved fusion proteins were purified further using an HisTrap column (GE Healthcare). Monomers of heparin-binding domains were dimerized at Cys^{65} by adding 1 mM DTT and dialyzing against Tris buffer (20 mM Tris and 150 mM NaCl; pH 8.0) for 48 h. Monomers and dimers were separated using an HisTrap column (GE Healthcare), and dimers were dialyzed against PBS before storage. Fibrinogen fragments were verified as >99% pure by SDS/PAGE and MALDI-TOF.

Detection of GF Binding to Fibrin(ogen) Fragments. As in the detection of GF binding to fibrinogen, ELISA plates were coated with 50 nM GFs and blocked. Then wells were incubated with Fg β1–$66_{(2)}$ or GST-fibrinogen fragments (in PBS-T with 0.1% BSA) for 45 min at room temperature. After three washes with PBS-T, wells were incubated with anti-His tag (ab1187; Abcam) or anti-GST tag (GE Healthcare) antibody conjugated to HRP for 45 min. Wells were then washed three times with PBS-T, and antibody was detected with tetramethylbenzidine substrate by measuring the absorbance at 450 nm.

Inhibition of GF–Fibrinogen Binding by Fg β15–$66_{(2)}$. ELISA plates were coated with 100 nM fibrinogen overnight at room temperature, and further blocked with 2% BSA in PBS-T for 1 h at room temperature. Then wells were washed with PBS-T and further incubated with 5 nM of GF (in PBS-T with 0.1% BSA) with increasing concentrations of Fg β15–$66_{(2)}$ for 45 min at room temperature. After three washes with PBS-T, bound GFs were detected using biotinylated antibodies (R&D Systems).

Surface Plasmon Resonance. Measurements were made with a Biacore X100 surface plasmon resonance (SPR) system (GE Healthcare). Fg β15–$66_{(2)}$ was immobilized via the C-terminal 6X His tag on a Ni^{2+} ion-complexed chip (XanTec Bioanalytics) for ∼500 resonance units (RU) according to the manufacturer's instructions. Running buffer (0.1% BSA in PBS-T) was flowed onto the channels until the baseline stabilized and reached 100–150 RU. GFs were flowed at increasing concentrations (1.28–100 nM) in the running buffer at 30 μL/min. Specific binding of GFs to Fg β15–$66_{(2)}$ was calculated automatically using the response to a nonfunctionalized channel as a reference. Experimental results were fitted with Langmuir binding kinetics using BIAevaluation and Biacore X100 software (GE Healthcare).

Inhibition of Fg β15–$66_{(2)}$–GF Binding by Heparin. ELISA plates were coated as for the binding of Fg β15–$66_{(2)}$ to GFs. Then wells were washed with PBS-T and further incubated with 10 nM Fg β15–$66_{(2)}$ (in PBS-T with 0.1% BSA) for 45 min at room temperature with increasing concentrations of heparin (0-100 μM). The wells were washed three times with PBS-T and then incubated with anti-His tag antibody conjugated to HRP (ab1187; Abcam) for 45 min. After three washes with PBS-T, antibody was detected with tetramethylbenzidine substrate by measuring the absorbance at 450 nm.

Proliferation Assay. Proliferation assays were performed using starved human endothelial cells from umbilical vein (passage 3; PromoCell) in MCDB-131 medium (Invitrogen) containing 2% FBS. Cells were plated on 96-well plates (3,000 cells/well) for 6 h in serum-free MCDB-131. Then the medium was removed, and cells were further stimulated with new MCDB-131 medium with 2% (vol/vol) FBS containing a GF (10 ng/mL VEGF-A165, 25 ng/mL PlGF-2, or 5 ng/mL FGF-2) and 30 μg/mL fibrinogen or 1.25 μg/mL Fg β15–$66_{(2)}$ in excess. Cell numbers were quantified after 72 h using a CyQUANT assay (Invitrogen). Percent

proliferation increases over basal proliferation (without GF or Fg $\beta15–66_{(2)}$) were calculated.

Fibrin-Mimetic Matrix. Eight-arm poly(ethylene glycol) (PEG; molecular weight 40,000) was purchased from NOF. Divinyl sulfone was purchased from Sigma-Aldrich. PEG vinylsulfones (PEG-VS) were produced and characterized as described previously (2). The factor XIIIa substrate peptides Ac-FKGGVPMSMRGGERCG-NH_2 and H-NQEQVSPLERCG-NH_2 and the cell-adhesion ligand H-NQEQVSPLRGDSPG-NH_2 ($\alpha_2PI_{1–8}$-RGD) were obtained from GL Biochem. Ac-FKGGVPMSMRGGERCG-NH_2 and H-NQEQVSPLERCG-NH_2 were added to PEG-VS in 1.2-fold molar excess over VS groups in 0.3 M triethanolamine (pH 8.0) at 37 °C for 2 h. The reaction solution was subsequently dialyzed against ultrapure water for 7 d at 4 °C. After dialysis, the product (8-PEG-FKGGVPMSMRGGERCG and 8-PEG-NQEQVSPLERCG) was lyophilized. NMR was used to confirm the correct product structure. For activation of factor XIII, 200 U/mL Fibrogammin (Behring) was activated in the presence of 2.5 mM $CaCl_2$ with 2 U/mL thrombin for 30 min at 37 °C. Small aliquots of activated factor XIIIa were stored at −20 °C for further use. Matrices were formed by factor XIIIa cross-linking. The cross-linking reaction was performed in 50 mM Tris buffer (pH 7.6) containing 50 mM $CaCl_2$ and 10 U/mL factor XIIIa.

Release of GF from Fibrin-Mimetic Matrix. Fibrin-mimetic matrices (50 μL) were generated in 50 mM Tris buffer (pH 7.6) to obtain 1.75% (wt/vol) PEG, 40 μM $\alpha_2PI_{1–8}$-RGD, 10 μM $\alpha_2PI_{1–8}$-Fg $\beta15–66_{(2)}$, 10 U/mL factor XIIIa, 50 mM $CaCl_2$, 1 μg/mL FGF-2, 1 μg/mL PlGF-1, and 1 μg/mL PlGF-2. Fibrin gels were polymerized at 37 °C for 1 h and then transferred into 24-well Ultra Low Cluster plates (Corning) containing 1 mL of buffer (20 mM Tris·HCl, 150 mM NaCl, and 0.1% BSA; pH 7.4). A control well that served as 100% released control contained only the GFs in 1 mL of buffer. Every 24 h, buffers were removed, stored at −20 °C, and replaced with fresh buffer. For the 100% released control well, 20 μL of buffer was removed each day and stored at −20 °C. Matrices were digested at day 7 by adding 0.05 U of plasmin (Roche) to the release buffer. Cumulative release of GF was quantified by ELISA (DuoSet; R&D Systems), using the 100% released control as a reference. For the quantification of $\alpha_2PI_{1–8}$-Fg $\beta15–66_{(2)}$ release, the same process was used, but with a release buffer not containing BSA. $\alpha_2PI_{1–8}$-Fg $\beta15–66_{(2)}$ was detected by direct ELISA using the 6X His tag and anti-His tag antibody conjugated to HRP (ab1187; Abcam).

Wound Healing Model. C57BLKS/J-m/Lepr db (*db*/*db*) male mice, aged 10–12 wk at the start of the experiments, were used. In each mouse, the back was shaved, and four full-thickness punch-biopsy wounds (6 mm diameter) were created. Immediately afterward, fibrin matrices (80 μL; 10 mg/mL fibrinogen, 2 U/mL thrombin, 4 U/mL factor XIII, 5 mM $CaCl_2$, 200 ng of FGF-2, and/or 200 ng of PlGF-2) or fibrin-mimetic matrix (80 μL; 1.75% PEG conjugates, 40 μM $\alpha_2PI_{1–8}$-RGD, 10 μM $\alpha_2PI_{1–8}$-Fg $\beta15–66_{(2)}$, 10 U/mL factor XIIIa, 50 mM $CaCl_2$, 200 ng of FGF-2, and/or 200 ng of PlGF-2) were polymerized on the wounds. To avoid drying of the matrices, the wounds were covered with nonadherent dressing (Adaptic; Johnson & Johnson) and then with an adhesive film dressing (Hydrofilm; Hartmann). After 10 d, the mice were killed, and the wounds were harvested for histological analysis.

Histomorphometric and Immunohistochemistry Analyses of Wound Tissue Sections. An 8-mm-diameter area including the complete epithelial margins was excised. Wounds were cut on one edge and embedded. Histological analysis was performed on serial sections (20-μm cryosections and 4-μm paraffin sections) until the central portion of the wound was reached. The extent of reepithelialization and granulation tissue formation was measured by histomorphometric analysis of tissue sections (with H&E staining) using ImageJ software. For analysis of reepithelialization, the distance that the epithelium had traveled across the wound was measured, with the muscle edges of the panniculus carnosus serving as an indicator of the wound edges. Reepithelialization was calculated as the percentage of the distance of edges of the panniculus carnosus muscle. For granulation tissue quantification, the area covered by a highly cellular tissue was determined and normalized with the distance to muscle edges of the panniculus carnosus to obtain the area at the center of the wound. Cryosections, fixed with acetone and blocked with 10% (vol/vol) goat serum, were incubated overnight at 4 °C with primary antibodies against CD31 (clone MEC 13.3; BD Pharmingen) and desmin (clone D33; Dako). Alexa Fluor 488-conjugated anti-mouse and Alexa Fluor 594-conjugated anti-rat (Invitrogen) were used as secondary antibodies. The association area was determined by measuring the area positive for desmin within the dilated area positive for CD31 using ImageJ software (setting the dilate iteration parameter to 5).

1. Martino MM, et al. (2009) Controlling integrin specificity and stem cell differentiation in 2D and 3D environments through regulation of fibronectin domain stability. *Biomaterials* 30(6):1089–1097.

2. Lutolf MP, Hubbell JA (2003) Synthesis and physicochemical characterization of end-linked poly(ethylene glycol)-co-peptide hydrogels formed by Michael-type addition. *Biomacromolecules* 4(3):713–722.

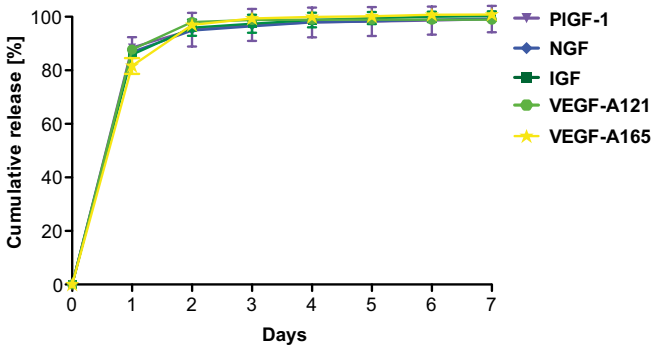

Fig. S1. Release of non/low–fibrinogen-binding GFs from fibrin matrix. Fibrin matrices were produced in the presence of a GF and further incubated in eight volumes of physiological buffer for 7 d. The buffer was changed each day, and released GFs were quantified for each day. The cumulative release of GFs over 7 d is shown ($n \geq 3$; mean ± SEM).

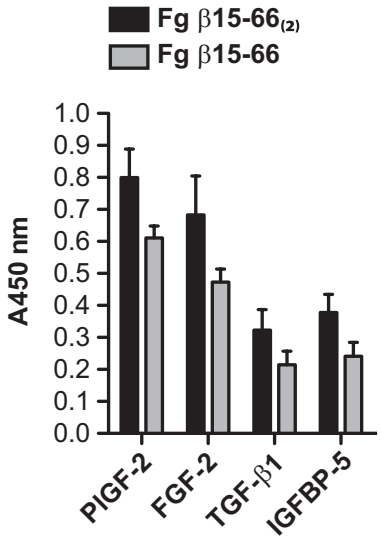

Fig. S2. GF binding to monomeric and dimeric Fg β15–66. ELISA plates were coated with GFs or BSA and further incubated with Fg β15–66 or Fg β15–$66_{(2)}$. Bound fibrinogen fragments were detected using an antibody against the His tag (n = 5; mean ± SEM).

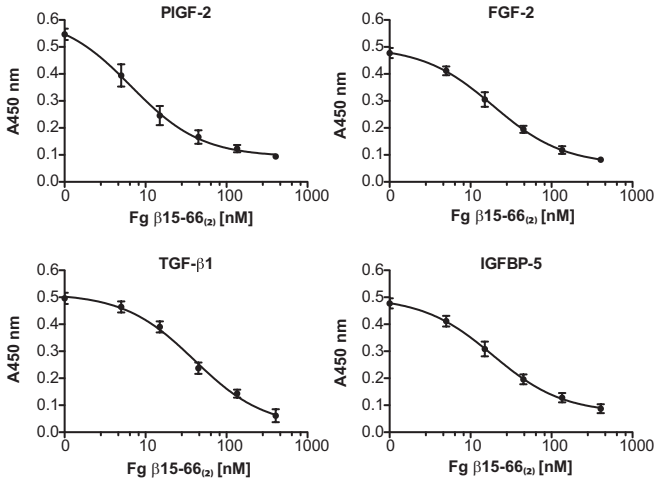

Fig. S3. Inhibition of GF binding to fibrinogen by Fg β15–$66_{(2)}$. ELISA plates were coated with fibrinogen or BSA and further incubated with GF solution containing Fg β15–$66_{(2)}$ at increasing concentrations (5–405 nM). Bound GFs were detected using a specific antibody for each GF (n = 3; mean ± SEM). The inhibition curve was fitted using log ([Fg β15–$66_{(2)}$]) vs. response, assuming a Hill slope of −1.0.

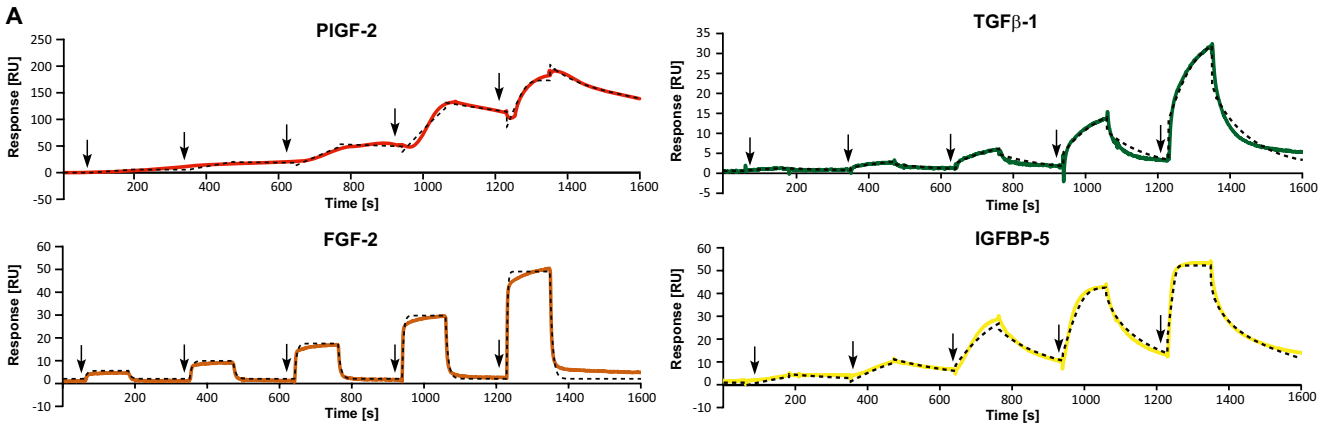

B

Fg β15-66$_{(2)}$

	PIGF-2	FGF-2	TGF-β1	IGFBP-5
K_D [nM]	1.9	53.0	56.5	19.6
k_{on} [1/Ms]	3.7 E+6	2.5 E+6	3.5 E+6	1.4 E+5
k_{off} [1/s]	7.2 E-3	1.3 E-1	1.8 E-2	2.8 E-3

C

FN III12-14

	PIGF-2	FGF-2	TGF-β1	IGFBP-5
K_D [nM]	3.1	10.6	14.6	2.0
k_{on} [1/Ms]	5.4 E+5	1.3 E+6	2.6 E+5	7.7 E+5
k_{off} [1/s]	3.1 E-4	1.5 E-2	2.1 E-3	1.4 E-3

Fig. S4. Affinity of selected GFs for Fg β15–66$_{(2)}$, estimated by SPR. SPR chips were functionalized with Fg β15–66$_{(2)}$ (~100–150 RU), and GFs were flowed over the chips at various concentrations (1.28–100 nM; black arrows). (*A*) Curves represent the specific responses (in RU) to Fg β15–66$_{(2)}$ obtained. Fits of experimental curves with Langmuir binding kinetics are shown by black dotted lines. (*B*) Table of binding kinetics values [dissociation constants (K_D) and rate constants (k_{on} and k_{off})] determined from the experimental curve fits. (*C*) Table of binding kinetics values to the second heparin-binding domain of fibronectin (FN III12–14) obtained previously (1).

1. Martino MM, Hubbell JA (2010) The 12th-14th type III repeats of fibronectin function as a highly promiscuous growth factor-binding domain. *FASEB J* 24(12):4711–4721.

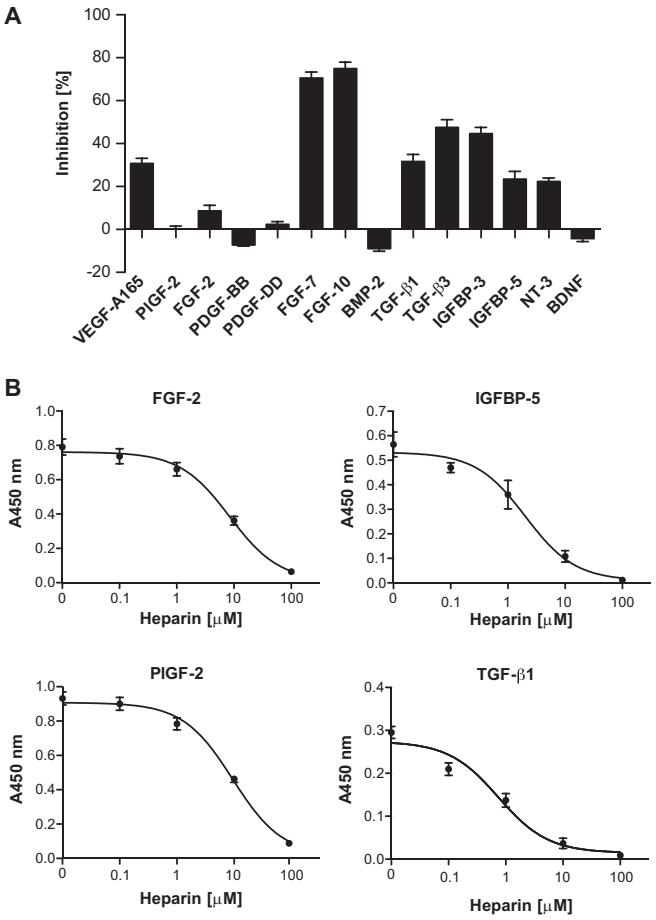

Fig. S5. Influence of heparin on GF–Fg $\beta15–66_{(2)}$ binding. (*A*) Graph showing the decrease in fibrinogen-binding signal to GFs when incubated with heparin in excess (20-fold molar excess relative to Fg $\beta15–66_{(2)}$) ($n = 3$; mean ± SEM). (*B*) Graphs showing the binding signal of Fg $\beta15–66_{(2)}$ to GFs when incubated with heparin at increasing concentrations (10- to 10,000-fold molar excess relative to Fg $\beta15–66_{(2)}$). The inhibition curve was fitted using log ([heparin]) vs. response, assuming a Hill slope of −1.0.

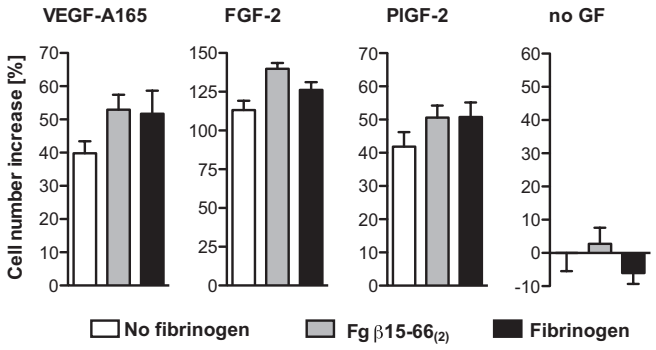

Fig. S6. GF activity in the presence of fibrinogen or Fg $\beta15–66_{(2)}$. Proliferation of human endothelial cells was stimulated with various GFs (VEGF-A165, PlGF-2, and FGF-2) with or without fibrinogen or Fg $\beta15–66_{(2)}$ in excess (≥100-fold molar excess relative to GFs). The graphs show the increase in proliferation over baseline after 72 h (i.e., proliferation without either GF or Fg $\beta15–66_{(2)}$). GFs significantly increased cell proliferation, but no synergistic effect was noted between cells treated with GFs alone and cells treated with GFs plus fibrinogen or Fg $\beta15–66_{(2)}$ (Student *t* test; $n = 3$; mean ± SEM).

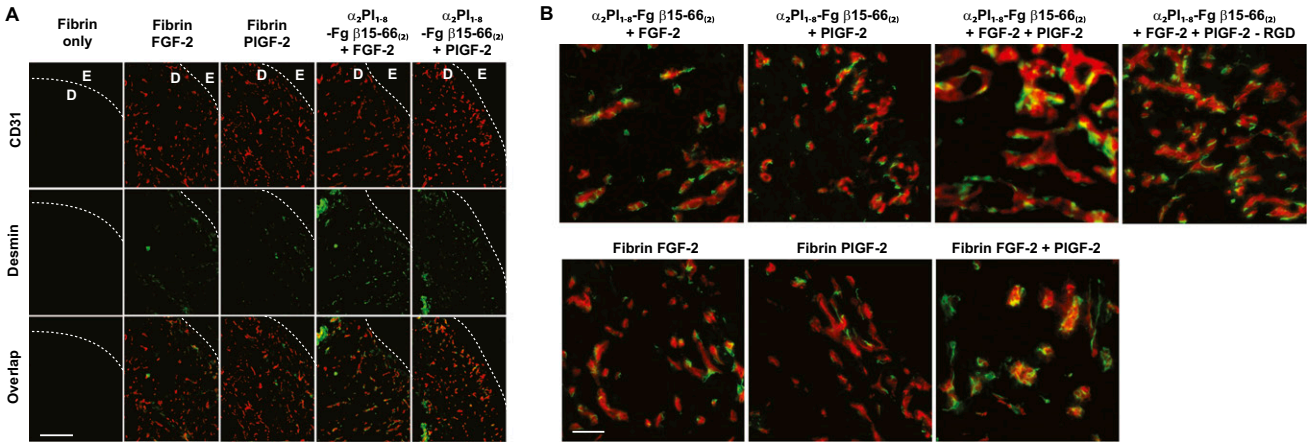

Fig. S7. Angiogenesis within the granulation tissue. Angiogenesis was revealed by staining for endothelial ($CD31^+$) cells and smooth muscle (desmin-positive) cells. (*A*) Representative images are shown. E, epidermis; D, dermis. The hashed line indicates the basement membrane. (Scale bar: 0.2 mm.) (*B*) Focus on the colocalization of and anatomic relationship between $CD31^+$ and desmin-positive cells. (Scale bar: 50 μm.)